Application of FX Singular Spectrum Analysis on Structural Data

Summary

The application of the Singular Spectrum Analysis (SSA) method on seismic data has been extensively studied by researchers over the past number of years. Ulrych et al (1988) initially applied eigenimage filtering to seismic data. Trickett furthered this work by using frequency slices and extending eigenimage filtering to 3D data (Trickett, 2003, 2009). This poster studies the results of the SSA method when applied to noisy structural data. On both synthetic and real data, we show that the FX SSA filter (Cadzow filtering) preserves faults much better than the standard FX prediction filter (Canales, 1984). This poster discusses how the discontinuity in a plane wave would affect the rank of the trajectory matrix in SSA.

Introduction

The Singular Spectrum Analysis (FX SSA) method (Sacchi, 2009) has been widely used for analysis of time series in various fields outside geophysics such as meteorology, hydrology, sociology and economic forecasts, before being applied to seismic data processing. FX SSA is also known as Cadzow FX filter (Cadzow, 1988) or the Caterpillar method (Golyandina et. al., 2001, 2007). Trickett used SSA separately on frequency slices and furthered its application to 3D using FXY eigenimage filtering.

The purpose of this poster is to demonstrate on both synthetic and real data that the SSA method (FX Cadzow filter) works much better than standard FX in preserving dips, diffractions and faults on structured data.

Theory

The philosophy of Cadzow and Eigenimage filtering utilizes an approximation of the matrix A by another matrix A_r of a lower rank r. Figure 1 shows examples of a lower rank matrix approximation.

Figure 1. Examples of matrix approximation with lower rank matrix

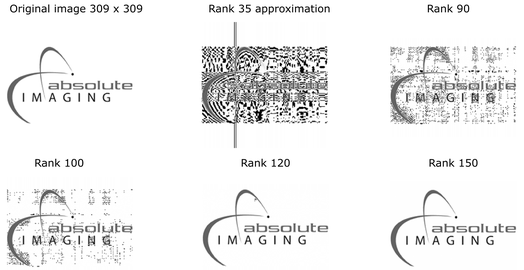

In seismic data processing these complex matrices are composed of Fourier coefficients of traces for each constant frequency slice. The difference between methods like Eigenimage, Cadzow, Hybrid and other rank-reduction filters is in how these corresponding traces are arranged in the frequency slice matrix.

1. Eigenimage filtering

$$\begin{bmatrix} a_{11} & a_{12} & a_{13} & \cdots & a_{1n} \\ a_{21} & a_{22} & a_{23} & \cdots & a_{2n} \\ a_{31} & a_{32} & a_{33} & \cdots & a_{3n} \\ \vdots & \vdots & \vdots & \ddots & \vdots \\ a_{m1} & a_{m2} & a_{m3} & \cdots & a_{mn} \end{bmatrix}$$

2. Cadzow filtering

$$\begin{bmatrix} a_{1} & a_{2} & a_{3} & \cdots & a_{n} \\ a_{2} & a_{3} & a_{4} & \cdots & a_{n+1} \\ a_{3} & a_{4} & a_{5} & \cdots & a_{n+2} \\ \vdots & \vdots & \vdots & \ddots & \vdots \\ a_{n} & a_{n+1} & a_{n+2} & \cdots & a_{2n-1} \end{bmatrix}$$

3. Hybrid (C^2) filtering

$$\begin{bmatrix} A_{1} & A_{2} & \cdots & A_{n} \\ A_{2} & A_{3} & \cdots & A_{n+1} \\ \vdots & \vdots & \ddots & \vdots \\ A_{n} & A_{n+1} & \cdots & A_{2n-1} \end{bmatrix}$$

where $A_i =$

$$\begin{bmatrix} a_{i,1} & a_{i,2} & \cdots & a_{i,n} \\ a_{i,2} & a_{i,3} & \cdots & a_{i,n+1} \\ \vdots & \vdots & \ddots & \vdots \\ a_{i,n} & a_{i,n+1} & \cdots & a_{i,2n-1} \end{bmatrix}$$

4. Hybrid (C^2) filtering—an example

$$\begin{bmatrix} a_{11} & a_{12} & a_{13} \\ a_{12} & a_{13} & a_{14} \\ a_{13} & a_{14} & a_{15} \end{bmatrix} \begin{bmatrix} a_{21} & a_{22} & a_{23} \\ a_{22} & a_{23} & a_{24} \\ a_{23} & a_{24} & a_{25} \end{bmatrix}$$

$$\begin{bmatrix} a_{21} & a_{22} & a_{23} \\ a_{22} & a_{23} & a_{24} \\ a_{23} & a_{24} & a_{25} \end{bmatrix} \begin{bmatrix} a_{31} & a_{32} & a_{33} \\ a_{32} & a_{33} & a_{34} \\ a_{33} & a_{34} & a_{35} \end{bmatrix}$$

In Eigenimage filtering (1) the corresponding traces for one frequency slice can be taken from any square grid such as a 3D stack or a cross-spread of prestack data. In Cadzow filtering the corresponding traces can come from a single shot gather ordered by offset or from 2D stack traces ordered by CDP. In Hybrid (C^2) filtering (Trickett, 2009) or 2D-extension (Golyandina et.al, 2007) block matrix A is composed of sub-matrices (A_i) which may be constructed from neighboring shot gathers. This increase in statistics improves the filter quality and does a better job at removing the random noise. To illustrate, example (4) shows three shots combined together to form matrix A.

Standard FX filter is based on an assumption that an ensemble of seismic traces has few linear events of constant dip and random noise. Therefore, FX filtering does not work well when the dip varies within the filter width or when there is a discontinuity of events within the filter width. Cadzow FX filtering does not have such limitations as it exploits another property – matrix rank. By increasing the rank we can approximate any complex structure.

Sacchi presented a simple explanation why in FX SSA the rank of the trajectory matrix $r=1$ for a plain wave (Sacchi, 2009). The plane wave is represented in *TX* and *FX* domain as $s(t,x)=w(t-px)$ and $S(w,x)=W(w)e^{-iwpx}$, where x is space coordinate, t – time, and w – angular frequency. For a regularly sampled coordinate $x=(k-1)\Delta x$, and for one fixed frequency, let $S_n=W e^{-i\alpha n}$, where $\alpha=wp\Delta x$.

For an example with 7 equally spaced traces, the trajectory matrix is

$$M=\begin{bmatrix} S_1 & S_2 & S_3 & S_4 \\ S_2 & S_3 & S_4 & S_5 \\ S_3 & S_4 & S_5 & S_6 \\ S_4 & S_5 & S_6 & S_7 \end{bmatrix} \qquad (1)$$

and by substitution of expression for S_n in M, Sacchi shows that this trajectory matrix has a rank $r=1$.

Following Sacchi, let us consider an example when our plain wave contains a discontinuity. Such a discontinuity can be simulated by dropping one trace from the series. So, instead of the plain wave series shown in Figure 2.a

$$S_1, S_2, S_3, S_4, S_5, S_6, S_7 \qquad (2)$$

let us consider

$$S_1, S_2, S_4, S_5, S_6, S_7, S_8 \qquad (3)$$

where S_3 is dropped so that all traces are shifted and a new trace S_8 is added to make the same number of traces (Figure 2.b)

Figure 2. Plain wave and plain wave with discontinuity

a. Plain wave

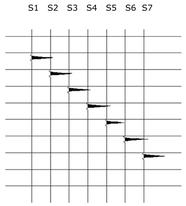

b. Plane wave with discontinuity – S3 omitted

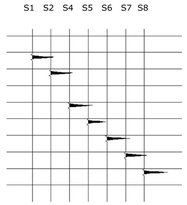

In the case of such a discontinuity, the trajectory matrix will look like

$$M=\begin{bmatrix} S_1 & S_2 & S_4 & S_5 \\ S_2 & S_4 & S_5 & S_6 \\ S_4 & S_5 & S_6 & S_7 \\ S_5 & S_6 & S_7 & S_8 \end{bmatrix} \qquad (4)$$

Let us compute the rank of such a trajectory matrix, when S_3 is skipped. For simplicity, let $y= e^{-i\alpha n}$, then $S_n=Wy^n$. Therefore,

$$M=\begin{bmatrix} S_1 & S_2 & S_4 & S_5 \\ S_2 & S_4 & S_5 & S_6 \\ S_4 & S_5 & S_6 & S_7 \\ S_5 & S_6 & S_7 & S_8 \end{bmatrix} = \begin{bmatrix} Wy & Wy^2 & Wy^4 & Wy^5 \\ Wy^2 & Wy^4 & Wy^5 & Wy^6 \\ Wy^4 & Wy^5 & Wy^6 & Wy^7 \\ Wy^5 & Wy^6 & Wy^7 & Wy^8 \end{bmatrix} \qquad (5)$$

After reduction of each line by its common factor (that will not change the rank), the matrix is

$$M_r = \begin{bmatrix} 1 & y & y^3 & y^4 \\ 1 & y^2 & y^3 & y^4 \\ 1 & y & y^2 & y^3 \\ 1 & y & y^2 & y^3 \end{bmatrix} \qquad (6)$$

Equation (6) shows that in this case the trajectory matrix has a rank $r=3$ (the 3rd and the 4th rows are the same and cannot be expressed as a linear combination of the 1st and 2nd rows).

Similarly, it is easy to show (by substitution of expressions for S_n and reducing the matrix to row echelon form) that when S_2 is dropped the rank of the corresponding trajectory matrix $r=2$; for S_4 $r=4$ etc., as shown in Table 1.

Table 1. Trajectory matrix rank versus fault location in a filter window

Omitted S_n number	2	3	4	5	6	7
rank	**2**	**3**	**4**	**4**	**3**	**2**

This means that if we have this type of discontinuity and use a running window for filtering, the minimum rank of the trajectory matrix sufficient for representing the traces would increase to its maximum as the centre of running window approaches the fault. However, in SSA we have the flexibility to approximate the trajectory with a matrix of higher ranks. The following synthetic examples demonstrate that even with a non-maximum rank, Cadzow FX method provides better results than the conventional FX.

Examples

The objective of the following synthetic examples was to find the limitations of both methods, FX and Cadzow FX, in preserving the resolution of complex structures including faults. No random noise was added since we were mostly interested in how well the structure is preserved after the filtering. Various parameters were tested for both the FX and Cadzow FX filters such as filter lengths, window lengths and rank.

Results of both methods FX and Cadzow FX depend on the selection of parameters. Bearing that in mind, we tested a range of parameter values for both methods to compare the best results of each. Figure 3 shows fault images at some tested window lengths and the numbers of samples for FX filtering and Figure 4 shows the same fault after application of Cadzow filter at different ranks and window lengths. The Cadzow filter shows some noise at the fault zone for 8 traces and rank 3 due to the ratio between the window length and the rank but all other results are better than the conventional FX filtering.

Figures 5 and 6 show the best results for both methods with the difference displays showing more signal removed with the FX filter than with the Cadzow FX filter, particularly in the faulted area. The real data examples shown in Figures 7-9 confirm the results found in the synthetic data and show better random noise attenuation when using the Cadzow FX filter.

Figure 3: F-X Filter

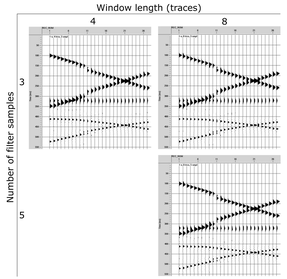

Figure 4: Cadzow Filter

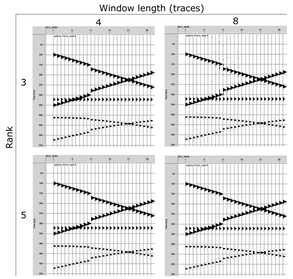

Figure 5: F-X Filter

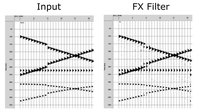

Figure 6: Cadzow Filter

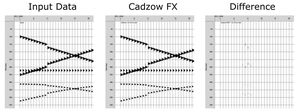

Figure 7: Structured Stack

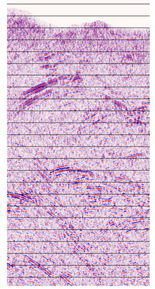

Figure 8: Structured Stack w FX

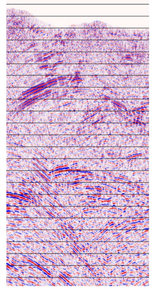

Figure 9: Structured Stack w Cadzow FX

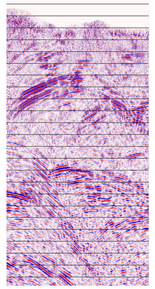

Seismic data for Figures 7—9 courtesy of: explor

Conclusion

The test results on the synthetic data show that the Cadzow FX method works better than the standard FX filter in preserving discontinuities. Our data examples also show an improvement when using the Cadzow FX filter. This is due to the fact that the FX filter assumes constant dips within the design window whereas the Cadzow is based on a matrix rank reduction using SVD resulting in better modeling of the complex structure.

References:

Cadzow, J., 1988, Signal Enhancement – A Composite Property Mapping Algorithm: IEEE Transactions on Acoustics, Speech and Signal Processing, 36, 49-62.

Canales, L.L., 1984, Random Noise Reduction: SEG, Extended Abstracts, 525-527.

Golyandina, N., Nekrutkin, V., and Zhigljavsky, A., 2001, Analysis of Time Series Structure: SSA and Related Techniques: CRC Press.

Golyandina, N., Usevich , K., and I.Florinsky, 2007, Filtering of Digital Terrain Models by two dimensional Singular Spectrum: International Journal of Ecology & Development, Vol. 8, No. F07, 81-94.

Sacchi, M. D., 2009, FX Singular spectrum analysis: CSPG CSEG CWLS Convention, Abstracts, 392-395.

Trickett, S. R., 2003, F-xy Eigenimage Noise Suppression, Geophysics, 68, 751-759.

Trickett, S., 2009, Prestack Rank-Reduction-Based Noise Suppression: CSEG Recorder, November, 24-31.

Ulrych, T., Freire, S., and Siston, P., 1988, Eigenimage Processing of Seismic Sections, SEG, Extended Abstracts 7, 1261.

Presented by:
Dr. Alexander Falkovskiy*, Elvis Floreani, Gerry Schlosser

absolute IMAGING

www.absoluteimaging.ca

Absolute Imaging Inc., Mission Centre, 2303 4th Street SW, Calgary, AB T2S 2S7